RSC Advances

REVIEW

Cite this: *RSC Adv.*, 2025, **15**, 10565

Five-membered heterocycles as promising platforms for molecular logic gate construction

Alexander Ciupa *

Received 1st February 2025
Accepted 28th March 2025

DOI: 10.1039/d5ra00749f

rsc.li/rsc-advances

The field of molecular logic gates began thirty years ago with the early pioneers de Silva *et al.* (A. P. de Silva, H. Q. N. Gunaratne and C. P. McCoy, *Nature*, 1993, **364**, 42) laying the foundation for modern molecular-scale switches and devices. Recent reports of lab-on-a-molecule and molecular calculators (Moleculators) demonstrate the potential of this bottom-up approach. Five-membered heterocycles were central to the first reported logic gates in 1994 and remain valuable scaffolds in the present day. This review provides an overview of logic gate design using Boolean logic, introduces the work of the first pioneers, and highlights recently reported five-membered heterocycle logic gates.

1 Introduction

The mid-20th century to modern day is often described as the information age due to technological advancement in the creation, processing, storage, and transmission of digital information.[1] The semiconductor transistor is the foundation of all modern electronics[2] performing various functions including switches alternating between ON and OFF voltage states. Combining multiple transistors enables complex calculations to be performed.[3,4] While early transistors were centimetres in size, modern transistors are nanometres enabling billions of transistors to be combined on a single microchip.[5] Society has benefited greatly from this miniaturization resulting in portable devices (smartphones and smartwatches) with processing powers unthinkable just two decades ago.[6] Moore's law famously states the number of transistors in an integrated circuit doubles every two years and this has historically been correct over the past 60 years (Fig. 1A).[10] In 2016 the electronic industry recognised current technological limits acknowledging new approaches were required to maintain increases in processing power (expressed as clock speed in Fig. 1A).[7,7b,10] The quest for miniaturization is not limited to transistors, the field of lab-on-a-chip[8] involves performing laboratory analysis on the microscale. Lab-on-a-chip devices include nuclear magnetic resonance (NMR) (Fig. 1B)[8b,c] and HPLC analysis (Fig. 1C).[9] This concept of miniaturization can be expanded to the molecular scale in the construction of molecular switches and devices. The ability to perform laboratory analysis at the molecular level, referred to as lab-on-a-molecule[11] validates this bottom-up approach. The first molecular-scale transistor[12a] was reported in 2009 with multiple reports of molecular-scale switches mimicking semiconductor transistors.[12b,c] As we reach the limits of current semiconductor transistors, advancement in the design and construction of atomic-scale devices to solve macroscale problems remains more critical than ever. While numerous chemical scaffolds have been adapted for molecular-scale switches and devices, this review will focus specifically on the five-membered heterocycles pyrazoline, pyrazole, imidazole, and pyrrole. These simple heterocycles are well suited for molecular logic gate construction due to their modular configuration, well-established fluorescence properties, and ease of synthesis from inexpensive commercially available starting materials. To provide a viable alternative to current semiconductor transistors, its essential molecular devices are manufactured on a cost-effective industrial scale. The five-membered heterocycles offer distinct advantages to achieve this research need. A general overview of molecular logic gate construction and an introduction to the early pioneers from the mid-1990s to recent developments will be discussed.

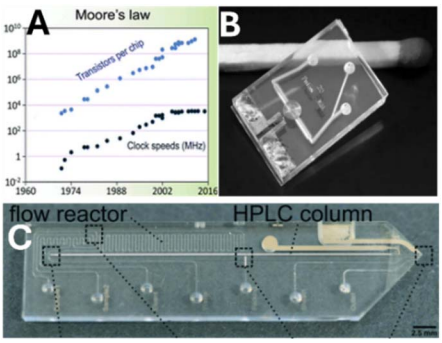

Fig. 1 Approaching the end of Moore's law (panel A),[7b] a lab-on-chip NMR (panel B)[8c] and HPLC (panel C).[9] Images reproduced from ref. 7*b*, 8*c* and 9 with permission from RSC, copyright 2019, 2005 and 2017 respectively.

Materials Innovation Factory, University of Liverpool, 51 Oxford Street, Liverpool L7 3NY, UK. E-mail: ciupa@liverpool.ac.uk

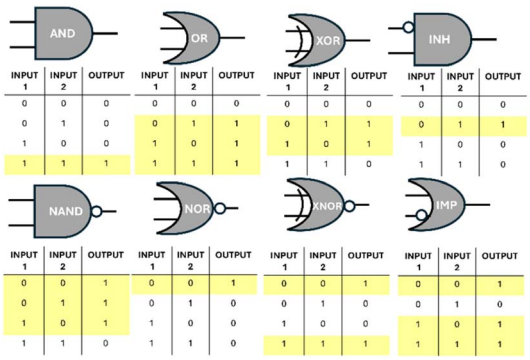

Fig. 2 Truth tables for basic logic gates using Boolean algebra.[13]

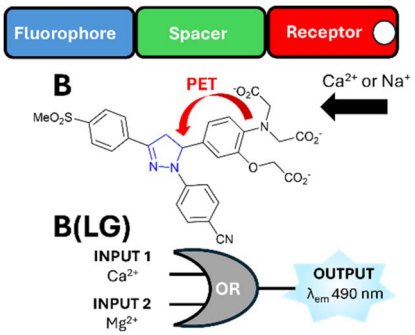

Fig. 4 Pyrazoline molecule **B** and its OR logic gate **B(LG)** application reported by de Silva *et al.*[16] in 1993.

2 Logic gates

In 1847 George Boole devised the foundation for computer science and the digital age, referred to as Boolean algebra.[13] This type of binary (0 or 1) algebraic logic is expressed as logic gates wherein an OUTPUT signal is triggered with specific INPUT configurations. These logical operations are expressed graphically in a truth table (Fig. 2). Combining multiple semiconductor transistor switches to create logic gates enables complex calculations to be performed. This process can be emulated using molecules in which the OUTPUT signal, typically fluorescence emission (λ_{em}), is triggered only in the presence of certain INPUT signals. This bottom-up approach could potentially overcome the technological limits of current semiconductor transistors. It is important to distinguish between the molecule itself and the logic gate properties derived from its response to the inputs. To that end, each logic gate will have the additional (LG) to highlight the logic gate properties which are mimicked under certain inputs. An AND logic gate only results in an OUTPUT of 1 if both INPUT 1 and INPUT 2 are present. Anthracene **A** with a crown ether attached *via* an amine spacer (Fig. 3) was reported in 1993 by de Silva *et al.*[14] Molecule **A** has two receptor units, the amine unit can bind to INPUT 1 (a proton) and the crown ether binds to INPUT 2 (a sodium ion). Upon excitation in the absence of both proton (H^+) and sodium ion (Na^+) photoelectron transfer (PET)[15] from either the amine or alkylbenzene unit (red arrows in Fig. 3) quenches fluorescence. The binding of a single input (either H^+ or Na^+) is not sufficient to fully deactivate the PET pathway. Both INPUT 1 and 2 are required to fully deactivate PET resulting in increased fluorescence (λ_{em}) at 428 nm. **A(LG)** was the first reported AND molecular logic gate.

An OR gate triggers an OUTPUT of 1 if either INPUT 1, 2, or both are 1. The first OR logic gate **B(LG)** (Fig. 4) was reported in 1994 by de Silva *et al.*[16] and is based on a fluorophore-space-receptor format around pyrazoline **B**. In the absence of either INPUT 1 (Ca^{2+}) or INPUT 2 (Mg^{2+}) the PET pathway quenches fluorescence (Fig. 4). The addition of Ca^{2+}, Mg^{2+}, or both deactivates PET resulting in "turn on" λ_{em} at 490 nm. While AND logic gate **A(LG)** operates in an organic medium, OR gate **B(LG)** operates in water at pH 7.3 suggesting logic gates could serve a valuable function for the detection of biologically important analytes in living systems. The opposite of an AND gate is a NOR gate, an OUTPUT of 1 is only triggered when both INPUT 1 and INPUT 2 are 0. A variety of different configurations are possible (Fig. 2) but the INHIBIT (INH) logic gate is of particular interest. In the INH gate an OUTPUT of 1 is triggered when INPUT 2 is present only (Fig. 2). If INPUT 2 and INPUT 1 are 1 then INPUT 1 inhibits the gate and the OUTPUT is 0. It is noteworthy to highlight the symbol for the INH gate is related to an AND gate with the addition of a small circle on the INPUT 1 line to symbolise the inhibitory function of INPUT 1. While useful as single units, combining logic gates allows sophisticated devices to be constructed. A molecular keypad lock[17] in which the INPUT signals must be entered in a particular order alongside molecular scale calculators[18] has been reported. These calculators, often referred to as Moleculators, can perform simple arithmetic using Boolean algebra. While numerous scaffolds have been used for logic gate construction,[19] this review will focus specifically on the five-membered heterocycles (Fig. 5).

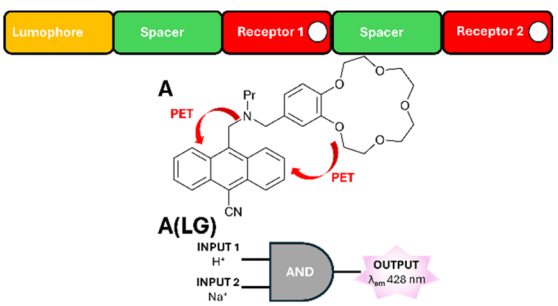

Fig. 3 Anthracene molecule **A** and its AND logic gate **A(LG)**.[14]

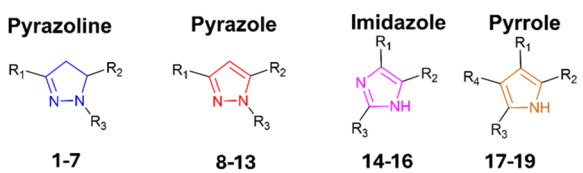

Fig. 5 Four different five-membered heterocycles used for logic gate construction.

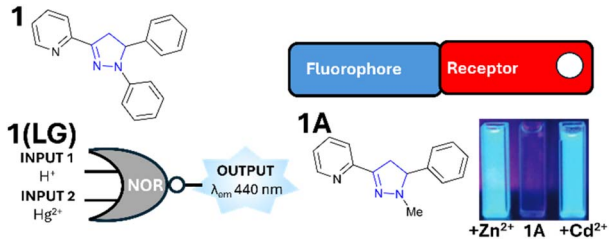

Fig. 6 Pyrazoline **1** and its NOR logic gate **1(LG)** application, pyrazoline **1A** with Zn^{2+} and Cd^{2+} image reproduced from ref. 23 with permission from RSC, copyright 2012.[23,24]

These simple scaffolds offer significant advantages in future molecular-scale switches and devices.

3 Pyrazoline-based logic gates

Pyrazolines, a five-membered non-aromatic heterocycle with two adjacent nitrogen atoms, are privileged structures[20] with a diverse range of medicinal applications.[21] Pyrazolines have well-established fluorescent properties[22] for logic gate construction. Pyridine-based pyrazoline **1** (Fig. 6) reported in 1999 by de Silva *et al.*[24] was the first NOR gate (combining a NOT and OR logic functions) with two inputs, proton (H^+) and mercury ions (Hg^{2+}). Logic gate **1(LG)** was designed according to the fluorophore-receptor system in which fluorescence output at λ_{em} 440 nm is present only in the absence of both INPUT 1 (H^+) and INPUT 2 (Hg^{2+}) (Fig. 6).[25] The presence of either or both INPUT quenched fluorescence. Pyrazoline **1** is a useful "turn on" fluorescence sensor for Zn^{2+} with λ_{em} 568 nm in MeCN.[25] Substitution of the N1 phenyl group in **1** for a methyl unit resulted in "turn on" sensor **1A** for both Zn^{2+} and Cd^{2+} at λ_{em} 460 nm in MeCN (Fig. 6) however no logic gate properties were reported.[23] Ferrocene-based pyrazolines **2** and **3** reported by Magri *et al.*[26] are designed according to the electron donor-spacer-fluorophore-receptor system (Fig. 7) as INHIBIT logic gates. In the absence of INPUT 1 (H^+) and INPUT 2 (Fe^{3+}) both **2** and **3** undergo photoelectron transfer (PET)[15] quenching fluorescence at λ_{em} 445 and 448 nm respectively. Addition of Fe^{3+} inhibited PET triggering fluorescence in the absence of H^+. At high H^+ (1 M H^+) there is approx. 40-fold decrease in quantum yield therefore both **2** and **3** are functioning as INHIBIT logic gates **2(LG)** and **3(LG)** (Fig. 7).

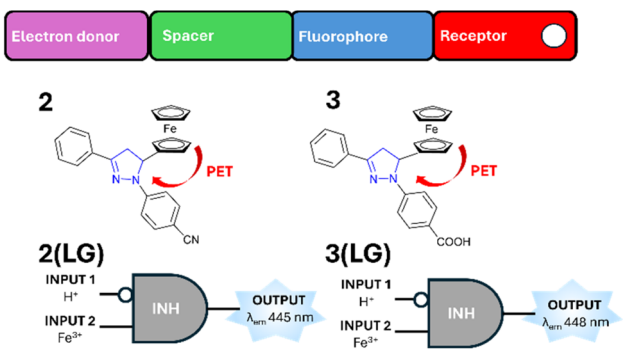

Fig. 7 Ferrocene-based pyrazoline **2** and **3** and their application as INHIBIT logic gates **2(LG)** and **3(LG)**.[26]

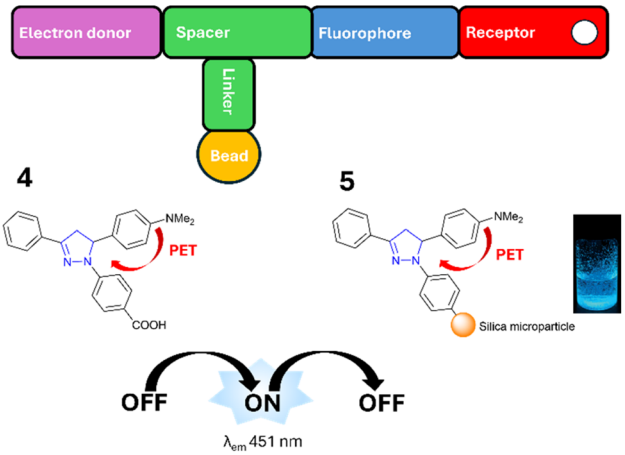

Fig. 8 Pyrazoline **4** and **5** off-on-off logic gates, image reproduced from ref. 28 with permission from RSC, copyright 2021.[28]

Sensors that detect pH and redox conditions are also known as Pourbaix sensors[27] with **2** and **3** leading examples. *N*,*N*-Dimethylaniline- based pyrazoline **4** was designed as an off-on-off ternary logic gate (Fig. 8) which would respond to various proton concentrations.[28] At low pH ($<10^{-3}$ M H^+) the PET[15] process is active quenching fluorescence (red arrows in Fig. 8). The carboxylic acid unit on **4** enabled the attachment of **4** to silica microparticles generating pyrazoline **5** (Fig. 8) *via* DCC coupling and amide bond formation.[28] Excitation of **5** resulted in blue fluorescence confirming attachment to microparticles was not detrimental to fluorescence (Fig. 8). This confirmed pyrazolines can be bound to solid substrates without loss of function, vital for industrial applications. Naphthalimide–pyrazoline **6** was an INHIBIT logic gate in which Fe^{3+} but not H^+ would trigger λ_{em} at 530 nm (Fig. 9).[29] In the presence of INPUT 2 (Fe^{3+}) PET[15] was inhibited triggering a "turn on" fluorescence response (Fig. 9). The addition of INPUT 1 (H^+) disrupted this process, therefore, **6(LG)** is an INHIBIT logic gate (Fig. 9). Pyrazoline **6** demonstrates combining the photophysical properties of naphthalimide with the rich electron ferrocene ring to fine-tune the desired logic gate properties.[29]

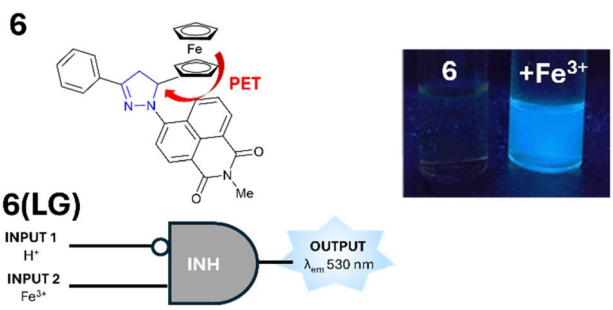

Fig. 9 Naphthalimide–pyrazoline **6** and its application as INHIBIT logic gate **(6LG)**, image reproduced from ref. 29 with permission from RSC, copyright 2022.[29]

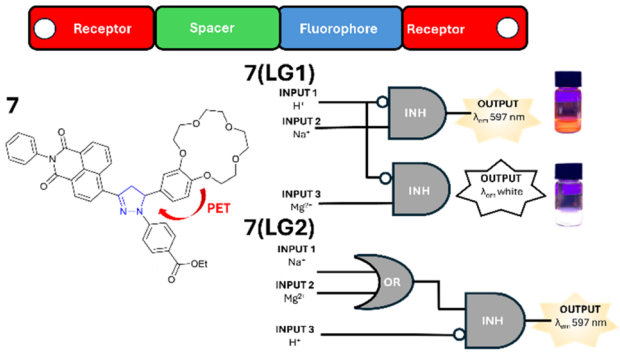

Fig. 10 Naphthalimide–pyrazoline with crown ether 7 and its application as logic gates 7(LG1) and 7(LG2), images reproduced from ref. 30 with permission from RSC, copyright 2023.[30]

A further naphthalimide–pyrazoline bearing a crown ether 7 was developed as a receptor-spacer-fluorophore-receptor system (Fig. 10).[30] The addition of the crown ether enables 7 to be receptive to biologically important metal ions, for example, sodium ions (Na^+) and magnesium ions (Mg^{2+}) enabling a range of different input signals to be used. In the absence of INPUT 1–3 (H^+, Na^+ or Mg^{2+}) PET is active from crown ether to pyrazoline (red arrows in Fig. 10), and no fluorescence is observed. On addition of INPUT 2 (Na^+) PET is inactive and λ_{em} 597 nm is observed (Fig. 10). On addition of INPUT 3 (Mg^{2+}) white light is observed. If INPUT 1 (H^+) is also present, then protonation of the N_2 on the pyrazoline ring reduces λ_{em}, and therefore 7 is acting as an INHIBIT logic gate 7**(LG1)**. In 7 the OUTPUT signal is dependent on INPUT allowing this structure to selectively detect Na^+ over Mg^{2+} at different wavelengths. An alternative configuration is an OR gate coupled with an INHIBIT gate to give 7**(LG2)** (Fig. 10). In this arrangement the presence of either INPUT 1 or 2 (or both) but in the absence of INPUT 3 (H^+) triggers OUTPUT 1. This unlocks the potential of 7 in medical applications involving the detection of biological metals at low pH. In summary, pyrazolines offer several advantages for the construction of logic gates (Fig. 11). Pyrazolines are easily synthesised from chalcone precursors enabling modular construction and orientation of specific R_1–R_3 groups around the pyrazoline ring. The pyrazoline is non-aromatic enabling activation and deactivation of the PET pathway. The N_2 on the pyrazoline has a lone pair of electrons which can act as a acceptor for H^+ ions enabling the sensing of different pH values (Fig. 11). Pyrazoline **5(LG)** validated the application to solid substrates[28] (Fig. 8), logic gate **6(LG)** demonstrated the advantages of combining different functional units[29] (Fig. 9),

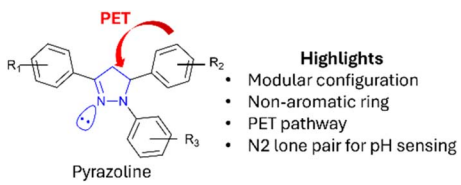

Fig. 11 Properties of pyrazoline heterocycles for logic gates.

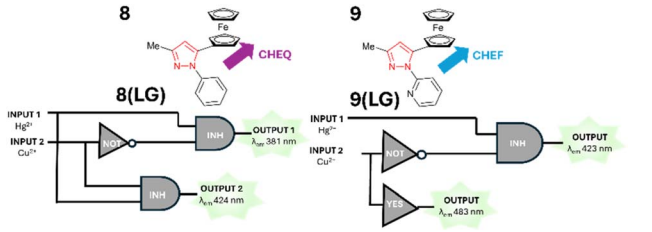

Fig. 12 Ferrocene-pyrazole 8 and 9 and their application as logic gates 8(LG) and 9(LG).[34,35]

and pyrazoline 7**(LG)** provided confirmation biologically relevant inputs (Na^+ and Mg^{2+}) can be utilised (Fig. 10).

4 Pyrazole-based logic gates

The pyrazole heterocycle, composed of an aromatic five-membered ring with two adjacent nitrogen atoms, is a privileged structure[31] present in a diverse range of biological applications.[32] Pyrazoles have unique fluorescence properties[33] valuable for logic gate applications. Ferrocene-based pyrazole **8** (Fig. 12) was designed for INHIBIT and NOR logic functions based on INPUT 1 (Hg^{2+}) and INPUT 2 (Cu^{2+}) ions (Fig. 12).[34] It is interesting to compare the structural similarity of **8** to ferrocene-pyrazoline logic gates **2**, **3** (Fig. 7), and **6** (Fig. 9) designed around a Fe^{3+} INPUT. In the presence of INPUT 1 only (Hg^{2+}) there is λ_{em} at 424 nm however if INPUT 2 is also present (Cu^{2+}) this fluorescence is reduced. In the presence of INPUT 2 (Cu^{2+}) only and not INPUT 1 (Hg^{2+}) then λ_{em} 381 nm is present. This logic gate approach was further developed in pyrazole **9** where the phenyl unit was replaced by a pyridine unit. Logic gate **9(LG)** is also designed around INPUT 1 (Hg^{2+}) and INPUT 2 (Cu^{2+}).[35] Of note is that ferrocene-based pyrazoles **8** and **9** operate around a chelation-enhanced fluorescence effect (CHEF) whereas ferrocene-based pyrazolines **2**, **3**, and **6** operate *via* disruption of the photoinduced electron transfer (PET) effect. This highlights that while pyrazolines and pyrazole are structurally very similar, the difference in aromaticity results in profoundly separate fluorescence mechanisms. Pyrazole **10** incorporating a pyridine unit was designed to function as an Al^{3+} sensor in MCF3, a breast cancer, cell line (Fig. 13).[36]

In the presence of INPUT 1 (Al^{3+}) only a fluorescence response at λ_{em} 500 nm is triggered (Fig. 13) due to the chelation-enhanced fluorescence (CHEF). If INPUT 1 (Al^{3+}) and INPUT 2 (picric acid, PA) are present then fluorescence is

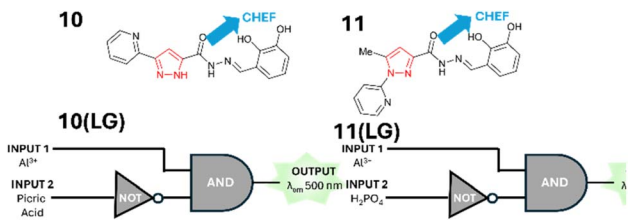

Fig. 13 Pyridine-based pyrazole 10 and 11 and their application as logic gates 10(LG) and 11(LG).[36,37]

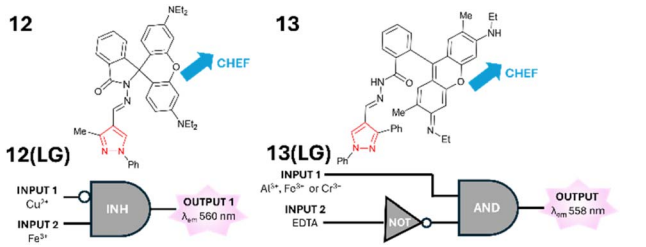

Fig. 14 Rhodamine-pyrazole **12** and **13** and their application as logic gates **12(LG)** and **13(LG)**.[38,39]

Fig. 15 Properties of the pyrazole heterocycle for logic gates.

inhibited (Fig. 12). Of note are the Al^{3+} limit of detection of 10^{-7} M and confirmation **10(LG)** operates *in vitro* demonstrating real-world applications. Pyridine-based pyrazole **11** (Fig. 13) was confirmed as logic gate **11(LG)** *in vitro* in H549, a lung cancer, cell line.[37] This logic gate performed an INHIBIT function with λ_{em} at 506 nm due to CHEF in the presence of INPUT 1 (Al^{3+}) only, when INPUT 2 (H_2PO_4) was present fluorescence was inhibited (Fig. 13). Rhodamine-pyrazole **12** displayed a fluorescence "turn on" response to a range of metals including Cu^{2+}, Fe^{3+}, Al^{3+} and Hg^{2+} in 1 : 1 MeCN : H_2O with λ_{em} approx. 560 nm (Fig. 14).[38] **12(LG)** functioned as an INHIBIT logic gate in the presence of INPUT 2 (Fe^{3+}) triggering a "turn on" response at 560 nm (Fig. 14). If INPUT 1 and INPUT 2 (Cu^{2+}) are present, then λ_{em} is disrupted. The ability to function in aqueous solution is a useful feature of **12**. Rhodamine-pyrazole **13** also displayed a "turn on" response to numerous metals including Al^{3+}, Fe^{3+}, and Cr^{3+} in 7 : 3 EtOH : H_2O solution with λ_{em} 558 nm due to CHEF (Fig. 14).[39] The INHIBIT logic gate **13(LG)** composed of NOT and AND functionality was constructed in which INPUT 1 was Al^{3+}, Fe^{3+} or Cr^{3+} and INPUT 2 was EDTA (Fig. 14). The ability to detect metals *in vitro* in SiHa, cervical cancer, cell line demonstrates real-world application of **13(LG)**. In summary, pyrazole-based logic gates have found real-world logic gate applications *in vitro*. Pyrazolines and pyrazole logic gates share the ability to incorporate different functional units around a central heterocycle core. This includes the addition of electron-rich ferrocene units, well-established chelators, or fluorescence dyes for optimised photophysical properties. Of note is pyrazole logic gates often differ in their fluorescence mode of action from pyrazolines and this must be factored into future design (Fig. 15).

5 Imidazole-based logic gates

Imidazole, a five-membered heterocycle with two nitrogen atoms separated by a carbon displays numerous biological

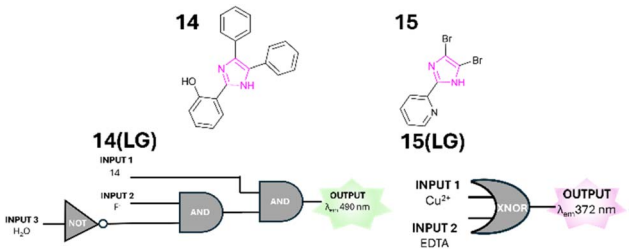

Fig. 16 Diphenyl-imidazole **14** and pyridine-imidazole **15** and their corresponding logic gates **14(LG)** and **15(LG)**.[41,42]

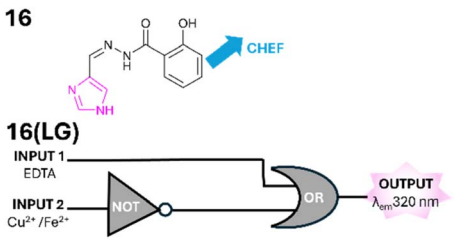

Fig. 17 Schiff base imidazole **16** and its logic gate **16(LG)**.[43]

properties.[40] Imidazoles are aromatic and more alike to pyrazole than pyrazolines. Simple diphenyl substituted imidazole **14** was a "turn on" sensor for the fluoride ion (F^-) with λ_{em} 490 nm in MeCN (Fig. 16).[41] Upon the addition of H_2O the "turn on" response is significantly reduced therefore **14** was developed as a water sensor that functions as logic gate **14(LG)**. Upon addition of INPUT 1 (**14**) and INPUT 2 (F^-) but not INPUT 3 (H_2O) both AND gates are satisfied, and OUTPUT is triggered at λ_{em} 490 nm (Fig. 16). If even small traces of H_2O are present the NOT gate is active closing the second AND gate disrupting OUTPUT. A real-world application of applying **14** to paper test strips and the detection of H_2O in a range of food products was confirmed. Brominated imidazole **15** was a "turn off" sensor for Cu^{2+} in DMSO (Fig. 16).[42] A XNOR logic gate **15(LG)** was constructed in which OUTPUT at λ_{em} 372 nm was only triggered in the absence of both INPUT 1 (Cu^{2+}) and INPUT 2 (EDTA) or the presence of both Cu^{2+} and EDTA (Fig. 16). The presence of just Cu^{2+} or just EDTA did not trigger λ_{em} 372 nm. Schiff base imidazole **16** is a "turn off" sensor for Cu^{2+} and Fe^{2+} in DMSO.[43] Logic gate **16(LG)** was constructed (Fig. 17) in which OUTPUT at 320 nm is only active in the presence of INPUT 1 (EDTA) or the presence of both INPUT 1 and INPUT 2 (ergo the NOT gate is satisfied). In this situation Cu^{2+} or Fe^{2+} are disrupting the CHEF however if EDTA is present this sequesters the metal ion (Fig. 17). In

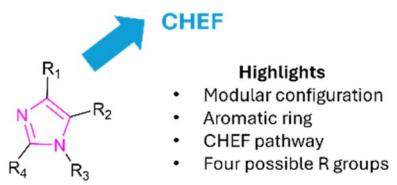

Fig. 18 Properties of the pyrazole heterocycle for logic gates.

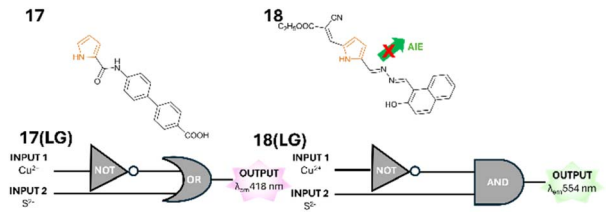

Fig. 19 Pyrrole **17** and **18** and logic gates **17(LG)** and **18(LG)**.[45,46]

summary, imidazole-based logic gates have been developed and found applications within *in vitro* studies. The fluorescence mode of action is primarily CHEF with a modular configuration around the heterocycle akin to pyrazoline and pyrazole logic gates (Fig. 18).

6 Pyrrole logic gates

Pyrrole is a five-membered aromatic heterocycle with a single nitrogen atom with multiple useful properties.[44] Pyrrole **17** is a "turn on" sensor for Al^{3+} and a "turn off" sensor for Cu^{2+} and Cd^{2+} in MeOH.[45] Logic gate **17(LG)** composed of a NOT and OR gate was structured (Fig. 19) and demonstrated in the absence of INPUT 1 (Cu^{2+}) there was fluorescence emission at λ_{em} 418 nm either with or without INPUT 2 (S^{2-}) (Fig. 19). The "turn off" response is triggered only in the presence of Cu^{2+}. Reversible binding was confirmed for **17** confirming it can be used for multiple cycles of detection (Fig. 19). Additional logic gates for Al^{3+} and Cd^{2+} were constructed and investigated.[45] The application of **17** to filter paper test strips for the detection of Al^{3+} in real-world environmental and industrial settings was suggested. Pyrazole **18** was also developed as logic gate **18(LG)** for the detection of Cu^{2+} using the inhibition of aggregation-induced emission (AIE) mode of action (Fig. 19).[46] A "turn off" response at 554 nm was detected either in the absence of INPUT 1 (Cu^{2+}) or the presence of both INPUT 1 and INPUT 2 (S^{2-}). **18** was applied to filter paper and suggested as a useful tool for the detection of Cu^{2+} in real-world applications.

Pyrrole **19** (Fig. 20) was initially designed as a phosphorescent probe for the fluoride ion (F^-) however further investigation revealed OR logic gate functionality for the hydroxide (OH^-) and acetate (AcO^-) ions (Fig. 20).[47] Upon addition of

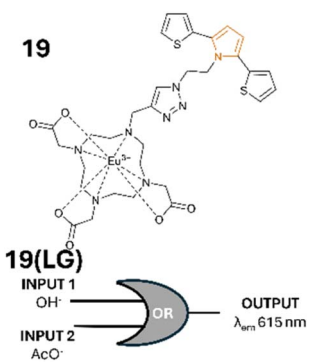

Fig. 20 Pyrrole-lanthanide complex **19** and its logic gate **19(LG)**.[47]

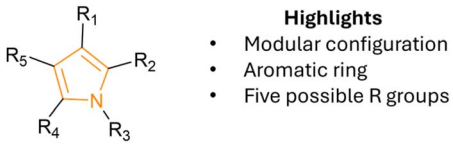

Fig. 21 Properties of the pyrrole heterocycle for logic gates.

hydroxide and acetate ions the emission bands at 615 nm and 700 nm increase due to binding to the Eu^{3+} centre (Fig. 20). The limit of detections for hydroxide and acetate were calculated as 0.7 μM and 0.87 μM in MeCN. Lanthanide based logic gates are rapidly emerging as a promising platform for logic gate design.[19d] While the number of pyrrole-based logic gates is currently low, this scaffold has potential for a range of unexplored metals such as the lanthanides (Fig. 21).

7 Conclusions

Multiple logic gates have been reported over the last thirty years[19] building on the pioneering work of de Silva *et al.* in 1993–4.[14,16] Magri *et al.* have expanded and advanced the pyrazoline scaffold further resulting in INHIBIT logic gates **2(LG)**, **3(LG)**, **6(LG)**, and **7(LG)** with useful applications.[26,28–30] The pyrazoline "turn on" fluorescence response operates *via* inhibition of the PET pathway[15] whereas the structurally related pyrazoles operate *via* CHEF or CHEQ. Numerous *in vitro* applications have confirmed pyrazoles can perform valuable operations within living systems for example **10(LG)**, **11(LG)**, and **13(LG)**.[36–39] Imidazole and pyrrole heterocycles have recently emerged as useful scaffolds for the development of logic gates enabling a range of previously unexplored inputs to be utilized. While pyrazoline and pyrazole inputs were typically based around proton (H^+) and metal ion (Hg^{2+}, Fe^{3+}, Mg^{2+}), imidazole and pyrrole logic gates **17(LG)**, **18(LG)** and **19(LG)** have expanded the range of inputs to other ions (S^{2-}, F^-, OH^- and AcO^-).[41–47] High throughput fluorescent screening platforms[48] enable multitudes of different inputs to be screened rapidly and efficiently. Recent developments in artificial intelligence and machine learning in drug discovery[49] could provide further insight into the development of heterocyclic logic gates. The algorithms developed for drug discovery could be modified for logic gate development resulting in highly unexpected logic gate designs and unusual inputs. While the last thirty years have firmly proven the concept of molecular scale devices, it's likely the next decade will focus on incorporating these cutting-edge technologies in the search for new logic gates to replace current semiconductor devices. The five-membered heterocycles provide many advantages and will be a valuable resource for the foreseeable future.

Data availability

No primary research results, software or code have been included and no new data were generated or analysed as part of this review.

Author contributions

Alexander Ciupa authored the manuscript.

Conflicts of interest

There are no conflicts to declare.

Acknowledgements

The Materials Innovation Factory, created as part of the UK Research Partnership Innovation Fund (Research England) and co-funded by the Sir Henry Royce Institute is acknowledged for providing funding.

References

1 N. Stafford, *Nature*, 2010, **467**, S19.
2 M. Li, H. Wu, E. M. Avery, Z. Qin, D. P. Goronzy, H. D. Nguyen, T. Liu, P. S. Weiss and Y. Hu, *Science*, 2023, **382**, 585.
3 M. S. Lundstrom and M. A. Alam, *Science*, 2022, **378**, 722.
4 C. Auth and A. Shankar, *IEEE Solid-St Circ. Mag.*, 2023, **15**, 20.
5 B. Dyatkin, *MRS Bull.*, 2021, **46**, 16.
6 D. Burg and J. H. Ausubel, *PLoS One*, 2021, **16**, e0256245.
7 Selected examples(*a*) T. N. Theis and H. S. P. Wong, *Comput. Sci. Eng.*, 2017, **19**, 41; (*b*) S. Gao, X. Yi, J. Shang, G. Liu and R.-W. Li, *Chem. Soc. Rev.*, 2019, **48**, 1531.
8 Selected examples(*a*) V. Narayanamurthy, Z. E. Jeroish, K. S. Bhuvaneshwari, P. Bayat, R. Premkumar, F. Samsuri and M. M. Yusoff, *RSC Adv.*, 2020, **10**, 11652; (*b*) Z. Li, Q. Bao, C. Liu, Y. Li, Y. Yang and M. Liu, *Lab Chip*, 2023, **23**, 1213; (*c*) H. Wensink, F. Benito-Lopez, D. C. Hermes, W. Verboom, H. Gardeniers, D. N. Reinhoudt and A. van den Berg, *Lab Chip*, 2005, **5**, 280.
9 J. J. Heiland, R. Warias, C. Lotter, L. Mauritz, P. J. W. Fuchs, S. Ohla, K. Zeitler and D. Belder, *Lab Chip*, 2017, **17**, 76.
10 M. M. Waldrop, *Nature*, 2016, **530**, 144.
11 Selected examples(*a*) D. C. Magri, G. J. Brown, G. D. McClean and A. P. de Silva, *J. Am. Chem. Soc.*, 2006, **128**, 4950; (*b*) K. Chen, Q. H. Shu and M. Schmittel, *Chem. Soc. Rev.*, 2015, **44**, 136; (*c*) G. J. Scerri, J. C. Spiteri, C. J. Mallia and D. C. Magri, *Chem. Commun.*, 2019, **55**, 4961; (*d*) M. Schmittel and H. W. Lin, *Angew. Chem., Int. Ed.*, 2007, **46**, 893.
12 Selected examples:(*a*) H. Song, Y. Kim, Y. H. Jang, H. Jeong, M. A. Reed and T. Lee, *Nature*, 2009, **462**, 1039; (*b*) I. Gallardo, G. Guirado, J. Hernando, S. Morais and G. Prats, *Chem. Sci.*, 2016, **7**, 1819; (*c*) P. Remon, S. M. Li, M. Grotli, U. Pischel and J. Andreasson, *Chem. Commun.*, 2016, **52**, 4659.
13 A. P. de Silva, *Molecular Logic-Based Computation*, Royal Society of Chemistry, Cambridge, UK, 2013.
14 A. P. de Silva, H. Q. N. Gunaratne and C. P. McCoy, *Nature*, 1993, **364**, 42.
15 Selected examples(*a*) A. P. de Silva and R. A. D. D. Rupasinghe, *J. Chem. Soc., Chem. Commun.*, 1985, 1669–1670; (*b*) B. Daly, J. Ling and A. P. de Silva, *Chem. Soc. Rev.*, 2015, **44**, 4203; (*c*) A. P. de Silva, T. S. Moody and G. D. Wright, *Analyst*, 2009, **134**, 2385; (*d*) H. Niu, J. Liu, H. M. O'Connor, T. Gunnlaugsson, T. D. James and H. Zhang, *Chem. Soc. Rev.*, 2023, **52**, 2322; (*e*) D. C. Magri, *Coord. Chem. Rev.*, 2021, **426**, 213598.
16 A. P. de Silva, H. Q. N. Gunaratne and G. E. M. Maguire, *J. Chem. Soc., Chem. Commun.*, 1994, **10**, 1213.
17 D. Margulies, C. E. Felder, G. Melman and A. Shanzer, *J. Am. Chem. Soc.*, 2007, **129**, 347.
18 D. Margulies, G. Melman and A. Shanzer, *J. Am. Chem. Soc.*, 2006, **128**, 4865.
19 Selected examples(*a*) D. Wu, A. C. Sedgwick, T. Gunnlaugsson, E. U. Akkaya, J. Yoon and T. D. James, *Chem. Soc. Rev.*, 2017, **46**, 7105; (*b*) L. Liu, P. Liu, L. Ga and J. Ai, *ACS Omega*, 2021, **6**, 30189; (*c*) N. I. Georgiev, V. V. Bakov and V. B. Bojinov, *Molecules*, 2023, **28**, 6327; (*d*) S. Zanella, M. A. Hernandez-Rodriguez, R. A. S. Ferreira and C. D. S. Brites, *Chem. Commun.*, 2023, **59**, 7863.
20 B. Varghese, S. N. Al-Busa, F. O. Suliman and S. M. Al-Kindy, *RSC Adv.*, 2017, **7**, 46999.
21 A. Tiwari, A. Bendi and A. S. Bhathiwal, *ChemistrySelect*, 2021, **6**, 12757.
22 Selected examples(*a*) A. Ciupa, *RSC Adv.*, 2024, **14**, 34918; (*b*) Z. L. Gong, F. Ge and B. X. Zhao, *Sens. Actuators, B*, 2011, **159**, 148; (*c*) Y. P. Zhang, Q. Teng, Y. S. Yang, H. C. Guo and J. J. Xue, *Inorg. Chim. Acta*, 2021, **525**, 120469; (*d*) A. Ciupa, *RSC Adv.*, 2024, **14**, 3519.
23 A. Ciupa, M. F. Mahon, P. A. De Bank and L. Caggiano, *Org. Biomol. Chem.*, 2012, **10**, 8753.
24 A. P. de Silva, I. M. Dixon, H. Q. N. Gunaratne, T. Gunnlaugsson, R. Pamela, R. S. Maxwell and T. E. Rice, *J. Am. Chem. Soc.*, 1999, **121**, 1393.
25 P. Wang, N. Onozawa-Komatsuzaki, Y. Himeda, H. Sugihara, H. Arakawa and K. Kasuga, *Tetrahedron Lett.*, 2001, **42**, 9199.
26 G. J. Scerri, M. Cini, J. S. Schembri, P. Fontoura da Costa, A. D. Johnson and D. C. Magri, *ChemPhysChem*, 2017, **18**, 1742.
27 Selected examples(*a*) D. C. Magri, *Supramol. Chem.*, 2017, **20**, 741; (*b*) M. Vella Refalo, J. C. Spiteri and D. C. Magri, *New J. Chem.*, 2018, **42**, 16474.
28 N. Zerafa, M. Cini and D. C. Magri, *Mol. Syst. Des. Eng.*, 2021, **6**, 93.
29 D. Sammut, N. Bugeja, K. Szaciłowski and D. C. Magri, *New J. Chem.*, 2022, **46**, 15042.
30 D. C. Magri and A. A. Camilleri, *Chem. Commun.*, 2023, **59**, 4459.
31 M. A. Alam, *Future Med. Chem.*, 2023, **15**, 2011.
32 O. Ebenezer, M. Shapi and J. A. Tuszynski, *Biomedicines*, 2022, **10**, 1124.
33 Selected examples(*a*) A. Tigreros and J. Portilla, *RSC Adv.*, 2020, **10**, 19693; (*b*) S. Melo-Hernández, M.-C. Rios and J. Portilla, *RSC Adv.*, 2024, **14**, 39230; (*c*) A. Ciupa, *New J. Chem.*, 2024, **48**, 13900.
34 V. S. Elanchezhian and M. Kandaswamy, *Inorg. Chem. Commun.*, 2010, **13**, 1109.

35 V. S. Elanchezhian, E. Kasirajan, P. Muthirulan, P. Muthukrishnan and M. Kandaswamu, *J. Mol. Struct.*, 2024, **1313**, 138687.
36 S. Saha, A. De, A. Ghosh, A. Ghosh, K. Bera, K. S. Das, S. Akhtar, N. C. Maiti, A. K. Das, B. B. Das and R. Mondal, *RSC Adv.*, 2021, **11**, 10094.
37 B. Das, M. Dolai, A. Ghosh, A. Dhara, A. D. Mahapatra, D. Chattopadhyay, S. Mabhai, A. Jana, S. Dey and A. Misra, *Anal. Methods*, 2021, **13**, 4266.
38 S. Gond, P. Yadav, A. Singh, S. Garai, A. Shekher, S. C. Gupta and V. P. Singh, *Org. Biomol. Chem.*, 2023, **21**, 4482.
39 A. I. Said, N. I. Georgiev and V. B. Bojinov, *Spectrochim. Acta, Part A*, 2019, **223**, 117304.
40 A. Siwach and P. K. Verma, *BMC Chem.*, 2021, **15**, 12.
41 X. Yu, Y. Li, Y. Li, Y. Liu and Y. Wang, *Spectrochim. Acta A*, 2025, **326**, 125245.
42 Z. Ekmekcia, G. Yilmaz and E. Duman, *Chem. Phys.*, 2020, **532**, 110693.
43 J. M. Priya, H. D. Revanasiddappa, B. Jayalakshmi, A. Swamynayaka, M. Madegowda, M. Iqbal, C. Shivamallu and S. P. Kollur, *Polyhedron*, 2024, **260**, 117110.
44 V. Bhardwaj, D. Gumber, V. Abbot, S. Dhiman and P. Sharma, *RSC Adv.*, 2015, **5**, 15233.
45 V. Kumar, P. Kumar and R. Gupta, *RSC Adv.*, 2017, **7**, 23127.
46 B. Tharmalingam, O. Anitha, J. Aiswarya, T. Thiruppathiraja, S. Lakshmipathi and B. Murugesapandian, *J. Photochem. Photobiol., A*, 2023, **442**, 114757.
47 M. Bilmez, A. Degirmenci, M. P. Algi and F. Algi, *New J. Chem.*, 2018, **42**, 450.
48 (*a*) X. Fang, Y. Zheng, Y. Duan, Y. Liu and W. Zhong, *Anal. Chem.*, 2019, **91**, 482; (*b*) E. Farrant, *ACS Med. Chem. Lett.*, 2020, **11**, 1506; (*c*) M. Trobe and M. D. Burke, *Angew. Chem., Int. Ed.*, 2018, **57**, 4192.
49 Selected examples(*a*) J. Vamathevan, D. Clark, P. Czodrowski, I. Dunham, E. Ferran, G. Lee, B. Li, A. Madabhushi, P. Shah, M. Spitzer and S. Zhao, *Nat. Rev. Drug Discovery*, 2019, **18**, 463; (*b*) A. Blanco-González, A. Cabezón, A. Seco-González, D. Conde-Torres, P. Antelo-Riveiro, A. Piñeiro and R. Garcia-Fandino, *Pharmaceuticals*, 2023, **16**, 891; (*c*) R. Gupta, D. Srivastava, M. Sahu, S. Tiwari, R. K. Ambasta and P. Kumar, *Mol. Divers*, 2021, **25**, 1315.